Published OnlineFirst October 20, 2020; DOI: 10.1158/1535-7163.MCT-20-0055

HIV Protease Inhibitors Block HPV16-Induced Murine Cervical Carcinoma and Promote Vessel Normalization in Association with MMP-9 Inhibition and TIMP-3 Induction

Yaqi Qiu[1,2], Federica Maione[1,2], Stefania Capano[1,2], Claudia Meda[1,2], Orietta Picconi[3], Serena Brundu[1,2], Alberto Pisacane[4], Anna Sapino[4,5], Clelia Palladino[3], Giovanni Barillari[5], Paolo Monini[3], Federico Bussolino[6,7], Barbara Ensoli[3], Cecilia Sgadari[3], and Enrico Giraudo[1,2]

ABSTRACT

Antiretrovirals belonging to the human immunodeficiency virus (HIV) protease inhibitor (HIV-PI) class exert inhibitory effects across several cancer types by targeting tumor cells and its microenvironment. Cervical carcinoma represents a leading cause of morbidity and mortality, particularly in women doubly infected with high-risk human papillomaviruses (HR-HPV) and HIV; of note, combined antiretroviral therapy has reduced cervical carcinoma onset and progression in HIV-infected women. We evaluated the effectiveness and mechanism(s) of action of HIV-PI against cervical carcinoma using a transgenic model of HR-HPV–induced estrogen-promoted cervical carcinoma (HPV16/E2) and found that treatment of mice with ritonavir-boosted HIV-PI, including indinavir, saquinavir, and lopinavir, blocked the growth and promoted the regression of murine cervical carcinoma. This was associated with inhibition of tumor angiogenesis, coupled to downregulation of matrix metalloproteinase (MMP)-9, reduction of VEGF/VEGFR2 complex, and concomitant upregulation of tissue inhibitor of metalloproteinase-3 (TIMP-3). HIV-PI also promoted deposition of collagen IV at the epithelial and vascular basement membrane and normalization of both vessel architecture and functionality. In agreement with this, HIV-PI reduced tumor hypoxia and enhanced the delivery and antitumor activity of conventional chemotherapy. Remarkably, TIMP-3 expression gradually decreased during progression of human dysplastic lesions into cervical carcinoma. This study identified the MMP-9/VEGF proangiogenic axis and its modulation by TIMP-3 as novel HIV-PI targets for the blockade of cervical intraepithelial neoplasia/cervical carcinoma development and invasiveness and the normalization of tumor vessel functions. These findings may lead to new therapeutic indications of HIV-PI to treat cervical carcinoma and other tumors in either HIV-infected or uninfected patients.

Introduction

The DNA of high-risk human papillomaviruses (HR-HPV) is detected in approximately 90% of uterine cervical carcinomas, with HPV16 being the most prevalent HR-HPV type (1). Productive infection of the uterine cervical epithelium is found in low-grade cervical lesions, such as cervical intraepithelial neoplasia (CIN1/2), but is largely decreased in advanced dysplasia (CIN3), owing to deregulation of *HPV* gene expression associated with integration of the viral genome in the host cell chromosomes (1). Although 70%–80% of CIN1/2 regress spontaneously, a low fraction persists for long periods of time, and it has become increasingly evident that persistency of HR-HPV infection is the major risk factor for cervical carcinoma development (1, 2). This most likely reflects the increased chance of (stochastic) HPV DNA integration leading to upregulation of the HPV E6 and E7 oncoproteins that, in turn, bind to the p53 and pRb tumor suppressors promoting their degradation or inactivation, respectively (1, 3). Accordingly, persistent HPV infection is also the main risk factor for CIN/cervical carcinoma recurrence after excisional treatment (4, 5).

The recent advent of effective preventative vaccines against HR-HPV has raised hope for cervical carcinoma eradication. However, despite vaccination campaigns, HR-HPV infection is still the most common sexually transmitted disease worldwide, with an estimated global prevalence of 11.7% (6, 7). Preventative HPV vaccines, in fact, are ineffective against already established infections. As a consequence, cervical carcinoma remains the fourth most common cancer in women (the second in Africa), accounting for a large part of morbidity and mortality worldwide (8), with 2% projected increase in global burden by 2030 (6). These data point to the need of developing new treatments to block cervical carcinoma onset and progression.

[1]Laboratory of Tumor Microenvironment, Candiolo Cancer Institute, FPO-IRCCS, Candiolo, Turin, Italy. [2]Department of Science and Drug Technology, University of Turin, Candiolo, Turin, Italy. [3]National HIV/AIDS Research Center, Istituto Superiore di Sanità, Rome, Italy. [4]Pathology Unit, Candiolo Cancer Institute, FPO-IRCCS, Candiolo, Turin, Italy. [5]Department of Medical Science, University of Turin, Candiolo, Turin, Italy. [5]Department of Clinical Sciences and Translational Medicine, University "Tor Vergata," Rome, Italy. [6]Laboratory of Vascular Oncology, Candiolo Cancer Institute, FPO-IRCCS, Candiolo, Turin, Italy. [7]Department of Oncology, University of Turin, Candiolo, Turin, Italy.

Note: Supplementary data for this article are available at Molecular Cancer Therapeutics Online (http://mct.aacrjournals.org/).

C. Sgadari and E. Giraudo contributed equally as co-senior authors of this article.

Y. Qiu and F. Maione contributed equally to this article.

Corresponding Authors: Enrico Giraudo, Candiolo Cancer Institute, Fondazione del Piemonte per L'Oncologia (FPO), IRCCS, Strada Provinciale 142, Km 3.95, Candiolo, Turin 10060, Italy. Phone: 39-01-1993-3279; Fax: 39-01-1993-3524; E-mail: enrico.giraudo@ircc.it; and Cecilia Sgadari, Istituto Superiore di Sanità, National HIV/AIDS Research Center, Viale Regina Elena 299, 00161 Rome, Italy. Phone: 39-06-4990-6071; Fax: 39-06-4990-2504; E-mail: cecilia.sgadari@iss.it

Mol Cancer Ther 2020;19:2476–89

doi: 10.1158/1535-7163.MCT-20-0055

Published OnlineFirst October 20, 2020; DOI: 10.1158/1535-7163.MCT-20-0055

CIN incidence and aggressiveness are particularly dramatic in human immunodeficiency virus (HIV)/HPV doubly infected women (9). In fact, HIV infection leads to increased prevalence, acquisition, and persistence of HR-HPV infection (9). Furthermore, HR-HPV infection can persist in both HIV^+ and seronegative women even after excision of low-grade CIN, leading to an overall 6% disease recurrence (5).

In this context, recent epidemiologic studies showed that antiretroviral treatment in HIV^+ women reduces the incidence and progression of CIN and ultimately the incidence of invasive cervical carcinoma (9, 10), although most of these studies did not discriminated between HIV protease inhibitors' (HIV-PI) and HIV reverse transcriptase inhibitors' antitumor effect. Of note, previous evidence indicates that HIV-1 PIs, a class of antiretroviral drugs widely used in HIV^+ patients, exert direct antitumor effects, which are independent of their antiviral activity. In particular, HIV-PIs can impair endothelial and tumor cell capability of degrading the extracellular matrix (ECM; refs. 11–18). As a consequence, HIV-PIs block tumor invasion and angiogenesis, thus inhibiting the growth of different tumor models including Kaposi sarcoma, the most frequent tumor in HIV-infected individuals (11, 13–16, 19). HIV-PIs block tumor and endothelial cell invasion via the functional impairment of the matrix metalloproteinases (MMP), ECM-degrading proteolytic enzymes, which play a central role in tumor angiogenesis, invasion, and metastasis (11, 13–15, 17, 18, 20). Interestingly, the HIV-PIs saquinavir (SQV), ritonavir (RTV) and, to a lesser extent, indinavir (IDV), can inhibit the growth and invasion of cultured CIN cells. This outcome is, in turn, due to inhibition of both MMPs expression and activity through inactivation of the Akt/Fra-1 signaling pathway, which is, instead, activated by the HR-HPV oncoproteins E6/E7 (15, 19). These effects of HIV-PIs occur at drug concentrations comparable with those present in plasma of treated patients (12, 13, 17). Furthermore, at drug concentrations above the therapeutic peak levels (50–100 μmol/L), HIV-PI causes apoptosis in tumor cells of several tumor types, including cervical carcinoma (13, 17, 21, 22). Finally, phase II clinical trials have shown that use of HIV-PIs is safe and effective in classical (non-HIV associated) Kaposi sarcoma occurring in elderly people (23) and in CIN lesions developing in HIV-negative women (24).

On the basis of these findings, we have explored the effectiveness and mechanism(s) of action of HIV-PIs against cervical carcinoma. To this goal, we used a HPV16 E6/E7 transgenic mouse model of HPV-induced estrogen-promoted cervical carcinoma, which well recapitulates the natural stages of cervical carcinoma development (HPV16/E2 mice) and is widely used for the evaluation of anti-angiogenic and antitumor compounds (25). CIN progression in both human cervical carcinoma and HPV16/E2 mice is promoted by increasing the expression/activity of MMP-9 and VEGF both beneath the stromal/epithelial junction and within the tumor mass, which is directly correlated with tumor vessel density, as also observed in human lesions (17, 20, 25, 26).

Here, we show that treatment of HPV16/E2 mice with either first- (indinavir and saquinavir) or second-generation [lopinavir (LPV)] HIV-PIs blocks the growth and promotes the regression of cervical carcinoma. This effect was associated with inhibition of tumor angiogenesis, MMP-9 activity, and VEGF binding to VEGFR2, coupled with upregulation of tissue inhibitor of metalloproteinase-3 (TIMP-3). Because of these actions, HIV-PIs induced tumor vessel normalization and relieved tumor hypoxia in HPV16/E2 cervical carcinoma. These findings shed light on the molecular mechanisms of HIV-PIs antitumor effect and support the use of these drugs as new therapeutics against cervical carcinoma and other tumors in HIV-infected or noninfected patients.

Materials and Methods

HPV16/E2 mouse model

Generation of keratin 14 (K14)-HPV16 transgenic mice, maintained in the FVB/n background (Charles River Laboratories), and 17β-estradiol (E2) treatment for cervical carcinogenesis were reported previously (25, 27). Briefly, at 1 month of age, virgin, female HPV16/E2 mice, bred in the animal facility of Candiolo Cancer Institute (Candiolo, Turin, Italy), were anesthetized through isoflurane anesthesia and slow-release pellets that deliver 17β-estradiol at doses of 0.05 mg over 60 days (Innovative Research of America Inc.) were implanted below the dorsal back skin. Subsequent pellets were implanted at 3 and 5 months of age for a total of 6 months of hormone treatment (25, 27). All animal procedures were approved by the Ethical Committee of the University of Turin (Candiolo, Turin, Italy) and by the Italian Ministry of Health and were conducted in compliance with European laws and policies.

Mice treatment and tissue preparation

HPV16/E2 mice (10 mice/group) were treated daily for 4 weeks between the 5th and the 6th month of age with the same indinavir, saquinavir, or lopinavir formulations as used in HIV-infected patients, in association with ritonavir, commonly used in HIV-infected patients to increase the absorption and prolong the half-life of HIV-PIs or coadministered drugs. Indinavir (Merck Sharp & Dohme) or Saquinavir (Roche, 1.4 or 1 mg/day, respectively) in association with ritonavir (AbbVie, 0.68 mg/day), or lopinavir in coformulation with ritonavir (LPV/r, Abbott, 0.46 mg/0.11 mg/day), was administered by intragastric gavage diluted in 0.2 mL of saline solution, as described previously (11, 14). These doses were selected to compensate the fact that in mice the 4-week intragastric gavage can only be performed once per day, and were found to be well-tolerated in preliminary toxicity experiments in transgenic mice as well in nude mice (11, 14). The control group received the same volume of saline solution. Carboplatin (Sigma-Aldrich, 20 mg/kg) and paclitaxel (Sigma-Aldrich, 15 mg/kg, kindly provided by Dr. Dario Sangiolo, Medical Oncology Unity, IRCCS, Candiolo, Turin, Italy) were both administered weekly for 4 weeks by two separated intraperitoneal injections (0.1 mL each), in association with LPV/r given as described above. Mice were regularly monitored for changes in weight and health status. At the end of treatment, mice were euthanized by cervical dislocation after anesthesia (isoflurane, intraperitoneal injection) followed by CO_2 administration. Cervices were then excised, embedded in optimal cutting temperature (OCT) compound, and immediately frozen. The whole sample was serially cryo-sectioned (10 μm sections) and every fifth slide was subjected to hematoxylin and eosin staining for tumor grading in a blinded fashion, as described previously (28). The total tumor volume was determined by using the formula $V = 2/3 \times A \times Z$, where A is the largest cross-sectional area of the tumor as determined by imaging using a BX-60 Microscope (Olympus) equipped with a color Qicam Fast 1394-digital CCD Camera 12 bits (QImaging Corp.) and Z is the depth of the tumor, as determined through serial sections (25).

Human cervix specimens

Human cervical specimens [normal cervix, $n = 4$; low-grade dysplasia (CIN1), $n = 4$; high-grade dysplasia (CIN2/3), $n = 4$; and cervical squamous carcinoma (cervical carcinoma, $n = 4$)] were

Published OnlineFirst October 20, 2020; DOI: 10.1158/1535-7163.MCT-20-0055

obtained from women who underwent surgery without preoperative therapy at the Candiolo Cancer Institute, IRCCs-FPO (Candiolo, Turin, Italy) in 2019. The tissue specimens, derived from leftover of surgical samples to be discarded after the histologic diagnosis, were completely anonymized and recorded by disease stage. The study was conducted in accordance with the Code of Ethics of the World Medical Association (Declaration of Helsinki) and within the guidelines and regulations defined by the Research Ethics Committee for Human Biospecimen Utilization (Department of Medical Sciences—ChBU) of the University of Turin (Candiolo, Turin, Italy). Considering that no patients' data were used and that specimens were completely anonymized with no impact on patient care, no specific written informed consent was required by the competent ethics committee.

IHC analysis

IHC for collagen IV and TIMP-3 was performed on frozen sections from mice or formalin-fixed, paraffin-embedded human sections (10-μm thick), respectively. Paraffin sections were deparaffinized with xylene and rehydrated with decreasing concentrations of ethanol in water and antigen retrieval was achieved by heating sections in sodium citrate buffer (pH 6.0) for 7 minutes in a 750-W microwave oven, followed by 20 minutes of cooling at room temperature. Sections were then pretreated with 3% H_2O_2 for 20 minutes and blocked with serum-free Protein Block (Dako) for 1 hour at room temperature. Tissues were incubated with rabbit anti-collagen IV polyclonal antibody (ab6586, Abcam) or rabbit anti-TIMP-3 polyclonal antibody (PA5-70423, Invitrogen) overnight at 4°C. Samples were then washed and incubated for 1 hour with an anti-rabbit HRP-conjugated antibody (Dako) and antigens were revealed with 3,3-diaminobenzidine (Sigma-Aldrich) according to the manufacturer's instructions. Sections were counterstained with hematoxylin and visualized with a BX-60 Microscope (Olympus) equipped with a color Qicam Fast 1394-digital CCD Camera 12 bits (QImaging Corp.). The expression levels of collagen IV or TIMP-3 were quantified by ImageJ software by analyzing three fields/mouse (for collagen IV) or three fields/section (for TIMP-3).

Immunofluorescence analysis

Immunofluorescence analysis was performed on frozen sections (10 μm) that were air-dried, fixed in zinc-fixative [6.05 g Tris, 0.35 g $Ca(C_2H_3O_2)2$, 2.5 g $Zn(C_2H_3O_2)2$, 2.5 g ZnCl, and 3.8 mL HCl 37%] for 10 minutes, blocked in 3% BSA and 5% donkey serum in 1 × PBS as detailed previously (29, 30) and incubated for 1 hour at room temperature with the following primary antibodies: rabbit anti-Ki67 mAb (1:100 dilutions, RM-9106, Thermo Fisher Scientific), rat anti-Panendothelial Cell antigen mAb (Meca32) (1:100, 550563, BD Pharmingen), rabbit anti-NG2 Chondroitin Sulfate Proteoglycan polyclonal antibody (1:100, AB5320, EMD Chemicon), rat anti-platelet–derived growth factor receptor (PDGFR)-α (1:100, 14-140182, e-Biosciences), goat anti-PDGFR-β (1:100, AF 1042, R&D Systems), rat anti-mouse F4/80 (1:100, MCA497GA, Bio-Rad), rabbit anti-cleaved caspase 3 mAb (1:100, 9664S, Cell Signaling Technology), rabbit anti-MMP-9 (N-terminal) polyclonal antibody (1:100, 10375-2-AP, Proteintech Group Inc), rabbit anti-TIMP-3 polyclonal antibody (1:100, PA5-70423, Invitrogen), and mouse GVM39 mAb specifically recognizing the VEGF:VEGFR2 complex (1:50, CD300, EastCoast Bio).The secondary antibodies used were conjugated to Alexa Fluor 555 or Alexa Fluor 488 Fluorochromes (1:200, Invitrogen). Cell nuclei were counterstained with DAPI (1:5,000, Invitrogen). All immunelocalization experiments were performed on multiple tissue sections (5 mice/treatment group) and included negative controls for determination of background staining.

Confocal microscopy and immunofluorescence quantifications

All immunofluorescence images were captured by using a Leica TCS SPE Confocal Laser-scanning Microscope (three fields/mouse, Leica Microsystems) and by maintaining the same laser power, gain, and offset settings. To quantify pericyte coverage (α-NG2, red channel or PDGFR-β, green channel) in each image, a region of interest (ROI) close to each blood vessel (Meca32, green channel or red channel for PDGFR-β) was selected and the fluorescence of the red and green channels was quantified using the Leica Confocal Software Histogram Quantification Tool (Leica Microsystems; ref. 30). The ratio of red to green channel mean fluorescence intensity was then calculated and values were expressed as the percentage of red to green costaining. A similar procedure, by using ImageJ software, was followed to quantify the apoptotic rate in endothelial cells by evaluating the colocalization ratio between caspase 3 (green channel) and Meca32 (red channel), to quantify the colocalization of the VEGF/VEGFR complex (red channel) and Meca32 (green channel), and to measure the colocalization ratio between TIMP3 (red channel) and Meca32 (green channel). The colocalization between TIMP-3 (red channel) and PDGFR-α or F4/80 (green channel) was quantified, as described above, by calculating the ratio between the two channels and values were expressed as percentage of red/green costaining. To determine the expression levels of Ki67 (red channel), caspase 3 (green channel), MMP-9 (green channel), and TIMP-3 (green channel), the fluorescence of three random ROIs of the same size was measured and values were normalized by comparing stained areas with the total cells present in that specific tissue area visualized by DAPI.

Tumor vasculature analysis

The surface area occupied by vessels was quantified through the Image-ProPlus 6.2 Software (Media Cybernetics; three fields/mouse), as described previously (30). Briefly, the area occupied by Meca32-positive structures was compared with the total tissue area visualized by DAPI. To analyze vessel branching and diameter, confocal images were analyzed with the imaging software winRHIZO Pro (Regent Instruments Inc.). This software reproduces vessel pattern, identifies vessel branching, and gives back forks (blood vessel branch points) per area. Branching was calculated as number of forks relative to total vessel area (three fields/mouse).

Tumor hypoxia analysis

The levels of tumor hypoxia were evaluated in cervical lesions of HIV-PI–treated and control mice 2 hours after intraperitoneal injection of 60 mg/kg pimonidazole hydrochloride (HP2-100 Hypoxyprobe Kit-Plus, Natural Pharmacia International Inc., 5 mice/group), as described previously (25, 29–31). Hypoxyprobe-1-Mab 1 FITC antibody (Chemicon/Millipore) was used on cervical frozen sections to detect the formation of pimonidazole adducts, according to the manufacturer's instructions. Confocal images were captured and analyzed by using confocal laser-scanning as described above, and pimonidazole quantification was performed by using the Leica Confocal Software Histogram Quantification Tool (three fields/mouse, Leica Microsystems).

In situ zymography

To evaluate the gelatinolytic activity within cervical lesions, an *in situ* zymography was performed on frozen sections from all treatment groups (25). Substrate was prepared by dissolving 1 mg DQ Gelatin (Thermo Fisher Scientific) in 1.0 mL Milli-Q water, and this was further diluted 1:50 in a reaction buffer containing 50 mmol/L

Published OnlineFirst October 20, 2020; DOI: 10.1158/1535-7163.MCT-20-0055

Tris-HCl, 150 mmol/L NaCl, 5 mmol/L $CaCl_2$, and 0.2 mmol/L sodium azide (pH 7.6). Tissue sections were coated with 250 μL of substrate, covered with parafilm, and incubated in a dark humidity chamber at 37°C for 2 hours. Sections were then rinsed with Milli-Q water and fixed in 4% neutral-buffered formalin for 10 minutes in the dark. Sections were then rinsed in PBS two times, for 5 minutes each, and mounted with glycerol containing DAPI to counterstain the nuclei. To verify the contribution of MMPs, control slides were preincubated with 20 mmol/L EDTA for 1 hour. Confocal images were captured, analyzed, and quantified by confocal laser-scanning as described above.

Real-time RT-PCR analysis

Total RNA was purified from pools of snap-frozen tissues (3 mice/treatment group) using TriReagent (Sigma-Aldrich) according to the manufacturer's instructions and quantified by the RNA 6000 Nano Assay kit in an Agilent 2100 Bioanalyzer (Agilent Technologies). Equal amounts (100 ng) of total RNA were reverse transcribed by High Capacity cDNA Archive Kit (Thermo Fisher Scientific). The samples were analyzed by using the following TaqMan Gene Expression Assays (Thermo Fisher Scientific) to detect the corresponding mouse transcripts: Mm00600163_m1 (for MMP-9), Mm01341361_m1 (for TIMP-1), Mm00441825_m1 (for TIMP-2), Mm00441826_m1 (for TIMP-3), and Mm01184417_m1 (for TIMP-4). Gene expression was quantitatively analyzed by using the ABI PRISM 7900HT Fast Real-Time PCR System (Thermo Fisher Scientific). Mouse TATA box protein probe (Mm01277042_m1) was employed as endogenous control detector for normalization. Similar results were obtained with GAPDH (Mm99999915_g1) as housekeeping gene. All measurements were performed in duplicates. Raw data were analyzed using the SDS2.2 Software (Applied Biosystems) to define relative quantity.

Statistical analyses

Student *t* test for independent samples or Wilcoxon–Mann–Whitney test was performed to evaluate differences between controls and each treatment group. Statistical analyses were carried out at two-sided with a 0.05 significance level, using SAS (version 9.4, SAS Institute Inc.).

Results

HIV-PIs block the progression of cervical cancer in HPV16/E2 mice

HPV16/E2 female mice were treated daily with HIV-PIs starting at the 5th month of age, when all animals show high-grade (CIN III) lesions or advanced tumors with a measurable mass (25, 28). In two independent sets of experiments, 10 mice per group received indinavir or saquinavir boosted with ritonavir (IDV/r or SQV/r), or LPV/r, respectively. A group of 10 animals receiving the buffer were the controls in both experiments. Animals were treated with HIV-PI doses comparable with those as employed in HIV-infected patients or patients with classical Kaposi sarcoma (11, 14, 23). After 1 month of treatment, mice were sacrificed and the tumor volume was measured. In the groups receiving IDV/r, SQV/r, or LPV/r, the tumor mass volume was reduced by 84%, 91%, and 91%, respectively, as compared with control mice ($P = 0.0002$; $P < 0.0001$; **Fig. 1A** and **B**). Strikingly, the mean tumor mass at the end of IDV/r, SQV/r, or LPV/r treatment was also significantly smaller than the tumor volume that was measured in HPV16/E2 mice at 5 months of age (representing the HIV-PI treatment starting point, $P = 0.0004$, $P = 0.0002$, and $P = 0.0003$, respectively), suggesting that these drugs efficiently promote tumor regression. Neither systemic nor organ toxicity was observed in treated animals.

To assess the mechanisms underlying the observed antitumor effect of HIV-PIs, sections of cervical lesions of HIV-PI–treated or control mice were assessed for the expression of the Ki67 cell proliferation marker, which has a prognostic value for survival in women with cervical carcinoma (32). Results indicated that Ki67 expression was significantly decreased within the tumor mass of mice treated with IDV/r, SQV/r, or LPV/r as compared with controls, in which Ki67 was highly expressed in both the epithelial basal layer and within the tumor mass ($P < 0.0001$; **Fig. 1C** and **D**).

Together, these findings indicate that treatment with HIV-PI at doses comparable with those safely used in HIV-infected patients or patients with classical Kaposi sarcoma (11, 14, 23) efficiently blocks tumor progression and promotes tumor regression in HPV16/E2 mice without displaying any significant side effect.

HIV-PIs impair tumor angiogenesis in HPV16/E2 tumors in association with enhanced apoptosis

To evaluate whether the antitumor property of HIV-PIs was associated with an effect on the tumor microenvironment (TME), as observed in other tumor models (11, 12, 14, 18), we assessed the effect of treatment on the tumor vasculature. To this aim, sections of cervical lesions of treated or control mice were assessed by immunofluorescence for the pan-endothelial cell marker, MECA32. Treatment with IDV/r, SQV/r, or LPV/r reduced the vessel area by 44%, 41%, and 56%, respectively, as compared with controls ($P < 0.0001$ for all treatment groups; **Fig. 2A** and **B**). Interestingly, while the vasculature of control mice showed an altered morphology with irregular, dilated, and tortuous vessel, in HIV-PI–treated animals the vessel branching was markedly reduced and the lumen diameters appeared to be more regular (**Fig. 2A** and **B**).

Tumor treatment with angiogenesis inhibitors can result in apoptosis of both tumor cells and vessel endothelial cells (33). In-line with the observed antiangiogenic property of HIV-PIs, caspase-3 immunostaining indicated that IDV/r, SQV/r, or LPV/r treatment of HPV16/E2 mice significantly increased the apoptosis of cervical lesions in HPV16/E2 mice ($P < 0.0001$, for all treatment groups; **Fig. 2C**). Moreover, confocal analysis demonstrated a statistically significant increase of apoptosis in tumor-associated vasculature of treated mice as compared with controls ($P < 0.0001$; **Fig. 2D**). These results indicate that HIV-PI treatment hampers the survival of both tumor cells and tumor-associated endothelial cells.

HIV-PIs promote vessel normalization in HPV16/E2 cervical tumors and improve the antitumor effects of conventional chemotherapy

The inhibition of tumor angiogenesis and the reduction of vessel abnormality by HIV-PIs suggested that these drugs could induce vessel normalization, a process occurring in response to distinctive anti-angiogenic therapies that renders the tumor vasculature more efficient in delivering oxygen and drugs. Because the increase in pericyte coverage of blood vessels is a key marker of tumor vessel normalization (34–37), a double staining of tumor tissues for pericyte (NG-2) and endothelial (MECA32) cell markers was performed. Noteworthy, a 57%, 66%, and 82% increase in pericyte vessel coverage was observed in HPV16/E2 mice treated with IDV/r, SQV/r, and LPV/r, respectively, as compared with controls ($P < 0.0001$, for all treatment groups; **Fig. 3A** and **B**). A significant increase of pericyte coverage was also demonstrated by double staining of LPV/r-treated lesions with Meca32 and PDGFR-β^+, another pericyte marker, further

Published OnlineFirst October 20, 2020; DOI: 10.1158/1535-7163.MCT-20-0055

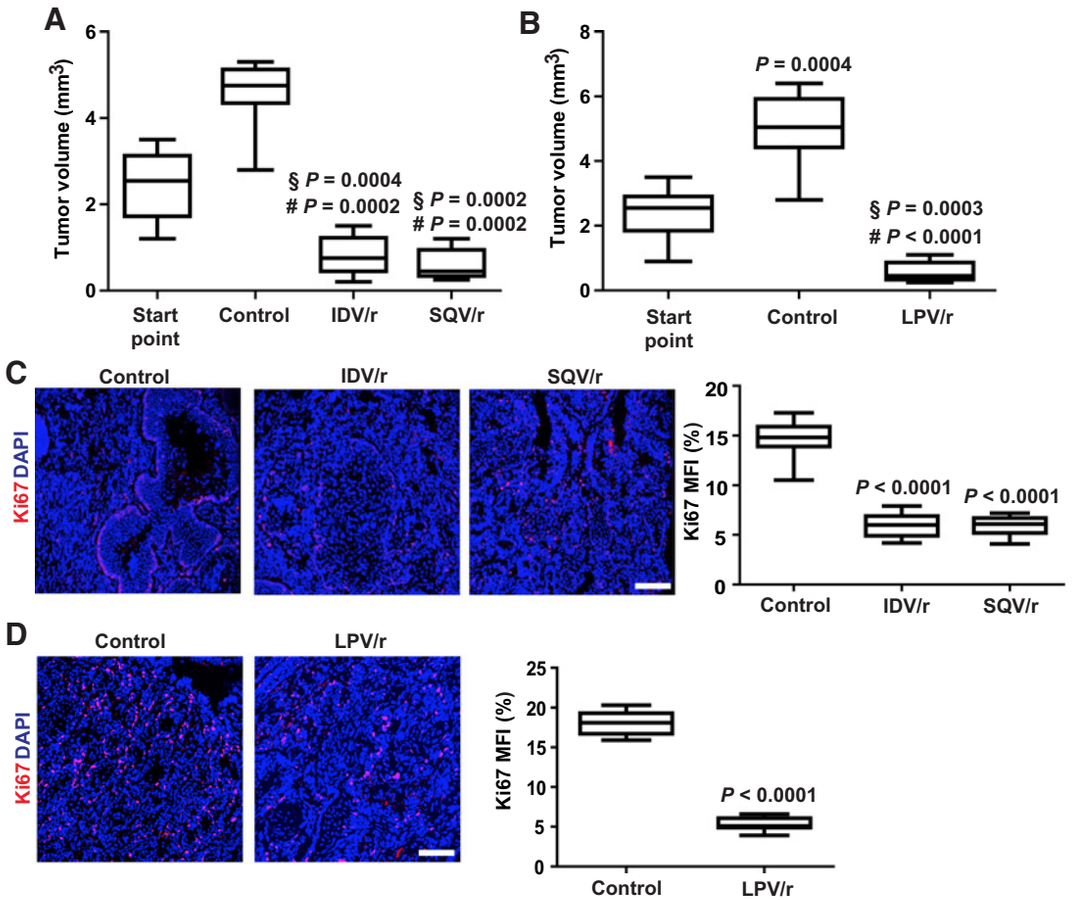

Figure 1.

HIV-PI treatment inhibits progression of cervical cancer and impairs tumor cell proliferation in HPV16/E2 mice. **A** and **B,** Box plots of cervical tumor mass evaluated using serial cervical sections (see Materials and Methods) from mice treated with IDV/r or SQV/r (**A**), or LPV/r (**B**), as compared with controls, sacrificed at the end of treatment (6 months of age) or at 5 months of age (treatment starting point) ($n = 10$ mice/group). A significant reduction of the tumor mass was evidenced in all treatment groups as compared with controls and with 5-month-old mice, by the unpaired Mann–Whitney U test (#, IDV/r, SQV/r, or LPV/r vs. control and §, IDV/r, SQV/r, or LPV/r vs. start point). **C** and **D,** Immunofluorescence staining of Ki67 (red channel) in representative cervical cross-sections from HPV16/E2 mice treated with IDV/r or SQV/r (**C**), or LPV/r (**D**), and controls mice (scale bars, 50 μm). The relative box plots show that the percentage of proliferating Ki67$^+$cells over the total tissue area was significantly decreased in mice treated with IDV/r, SQV/r (by 59%), or LPV/r (by 72%) compared with their respective controls. Results were analyzed by nonparametric two-tailed, unpaired Mann–Whitney U test ($n = 5$ mice/group).

indicating that indeed HIV-PI treatment increased the fraction of vessels associated with pericytes ($P < 0.0001$; Supplementary Fig. S1). Notably, a quantitative analysis of vessels stained with anti-Meca32 antibody by confocal microscopy, further demonstrated that HIV-PIs, by reducing the tumor vessel branching and diameters ($P < 0.0001$; **Fig. 3C** and **D**), indeed promote tumor vessel normalization. To assess whether the changes of tumor vessel phenotype were associated with an improvement of vessel functionality, hypoxia levels were evaluated in LPV/r-treated or control tumors by means of pimonidazole adduct immunostaining, a candidate biomarker of cancer aggressiveness (31). Remarkably, LPV/r treatment significantly decreased tumor hypoxia by 57% as compared with control mice ($P < 0.0001$; **Fig. 3E**).

Finally, to evaluate whether tumor vessel normalization promoted by HIV-PIs may enhance the delivery and the antitumor activity of the standard-of-care chemotherapeutic regimen in women with cervical carcinoma, tumor-bearing HPV16/E2 mice were treated weekly with carboplatin/paclitaxel in association with daily LPV/r, or with LPV/r or carboplatin/paclitaxel alone, for 4 weeks. Remarkably, when LPV/r was administered in association with carboplatin/paclitaxel, residual tumors were significantly smaller as compared with carboplatin/paclitaxel alone ($P = 0.0081$), LPV/r alone ($P = 0.0349$), or controls ($P = 0.0080$; **Fig. 3F**), without displaying additional toxicity. Of note, the tumor volume of LPV/r-treated mice was significantly smaller as compared with carboplatin/paclitaxel-treated animals ($P = 0.0082$), indicating that HIV-PIs have a more potent antitumor activity in HPV16/E2 mice than conventional chemotherapy (**Fig. 3F**). Altogether, these data indicate that HIV-PIs promote the normalization of tumor vasculature morphology and functionality.

HIV-PIs inhibit MMPs activity and reduce MMP-9 expression

We have previously demonstrated that the antiangiogenic and antitumor effects of HIV-PIs are due to blocking of MMPs expression and activation (11, 14, 15, 19). To investigate the molecular mechanism by which HIV-PIs exert their antiangiogenic and pronormalizing effect in HPV16/E2 mice, MMP activity was evaluated in cervical

Published OnlineFirst October 20, 2020; DOI: 10.1158/1535-7163.MCT-20-0055

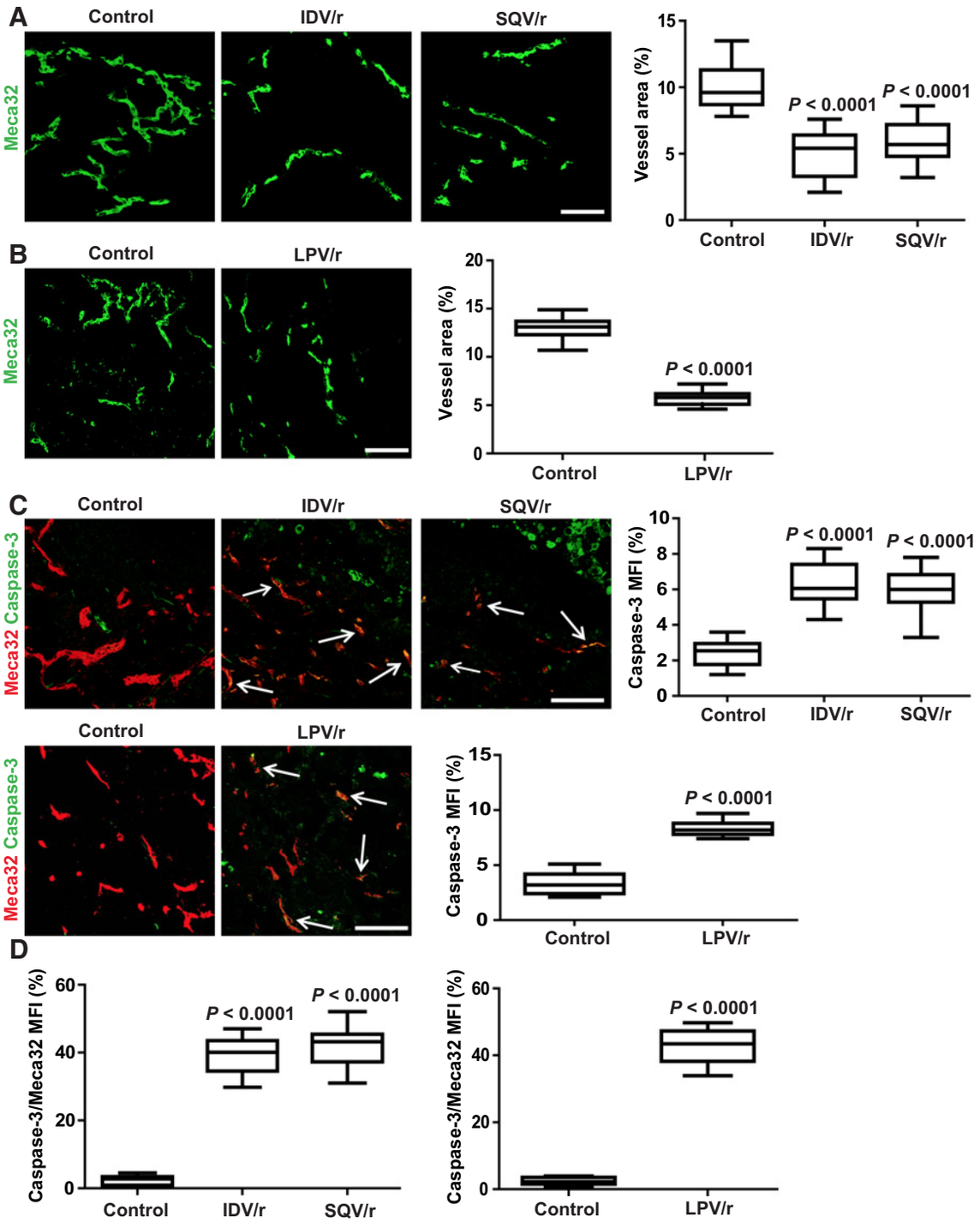

Figure 2.

HIV-PI treatment restrains tumor-associated angiogenesis in association with increased apoptosis in HPV16/E2 tumors. **A** and **B,** Confocal analysis of Meca32 (green channel) staining in representative HPV16/E2 tumors treated with IDV/r or SQV/r (**A**), or LPV/r (**B**), and control mice (scale bars, 50 μm). Box plots represent the percentage of Meca32-positive cells over the total tissue area for mice treated with IDV/r, SQV/r, or LPV/r, and respective controls. Results were analyzed by nonparametric two-tailed, unpaired Mann–Whitney U test ($n = 5$ mice/group). **C,** Immunofluorescence of caspase 3 (green channel) and Meca32 (red channel) in representative cervical cross-sections from mice treated with IDV/r, SQV/r, or LPV/r, and control mice (scale bars, 50 μm). Box plots show the rate of apoptotic (caspase 3^+) cells over the total tissue area for mice treated with IDV/r, SQV/r, or LPV/r, as compared with controls. A statistically significant increase of apoptosis of 2.6-, 2.4-, and 2.2-fold was detected in mice treated with IDV/r, SQV/r, or LPV/r versus controls, respectively. Results were analyzed by nonparametric two-tailed, unpaired Mann–Whitney U test, ($n = 5$ mice/group). **D,** Apoptotic endothelial cells' rate was quantified as the percentages of caspase 3 and Meca32 costaining (arrows). An increase of vessel apoptosis of 36.5%, 39.5%, and 40.5% was detected in mice treated with IDV/r, SQV/r, or LPV/r versus controls, respectively. Results were analyzed by nonparametric two-tailed, unpaired Mann–Whitney U test ($n = 5$ mice/group); scale bars, 50 μm.

Published OnlineFirst October 20, 2020; DOI: 10.1158/1535-7163.MCT-20-0055

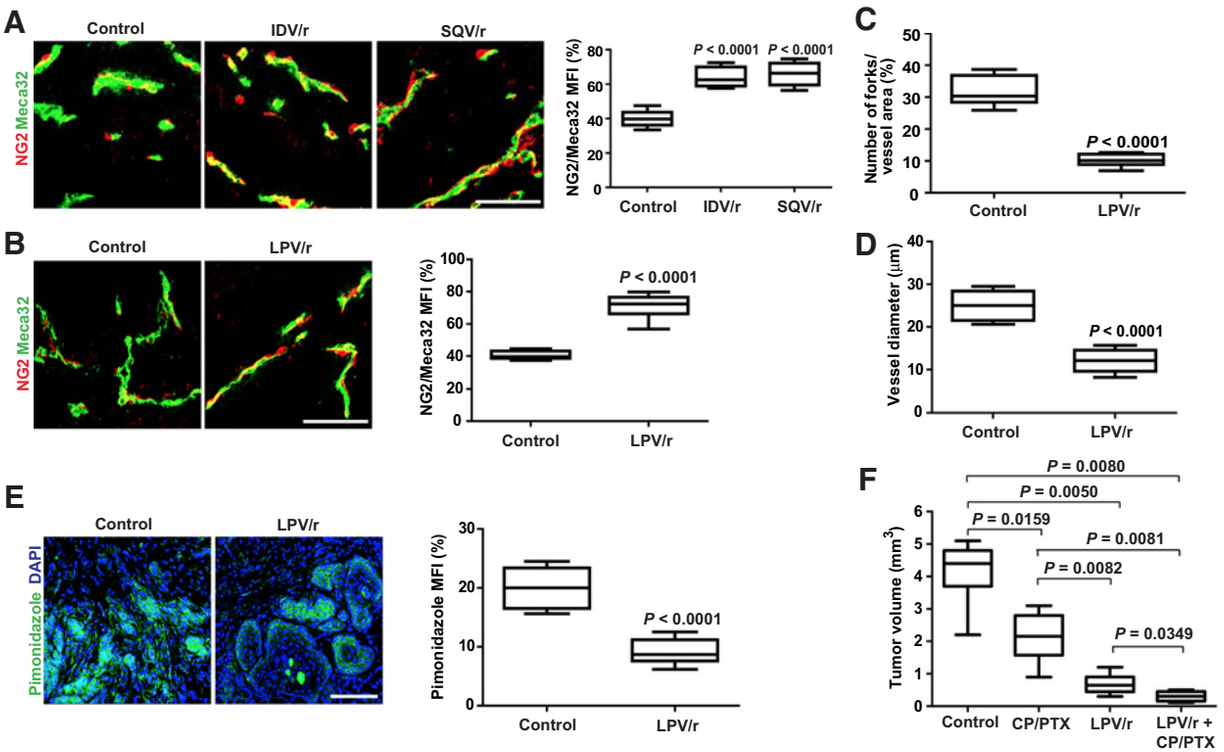

Figure 3.

HIV-PI treatment promotes tumor vasculature normalization and enhances antitumor effects of conventional chemotherapy in HPV16/E2 mice. **A** and **B,** Vascular pericyte coverage evaluated by immunostaining with Meca32 (green channel) and the pericyte marker, NG2 (red channel), in representative cervical cross-sections from HPV16/E2 mice treated with IDV/r or SQV/r (**A**), LPV/r (**B**), or controls (scale bars, 50 μm). The amount of pericyte coverage is presented as box plots of the percentages of NG2 and Meca32 costaining over the total Meca32-positive area. In mice treated with IDV/r, SQV/r, or LPV/r, pericyte coverage was significantly increased, as compared with controls. Results were analyzed by nonparametric two-tailed, unpaired Mann–Whitney U test ($n = 5$ mice/group). Confocal images of vessels stained with anti-Meca-32 antibody were used to quantify vessel branching (**C**) and diameters (**D**). Box plots show the reduction of vessel branching (by 67%) and vessel diameter (by 52%) in tumors treated with LPV/r compared with controls. Results were analyzed by nonparametric two-tailed, unpaired Mann–Whitney U test ($n = 5$ mice/group). **E,** Tumor hypoxia was assessed by means of pimonidazole adducts (green) immunofluorescence in serial sections of cervical tumors from mice treated with LPV/r or controls (scale bars, 50 μm). A significant decrease of hypoxia (by 57%) in lesions from LPV/r-treated mice as compared with controls was evidenced. Results were analyzed by nonparametric two-tailed, unpaired Mann–Whitney U test ($n = 5$ mice/group). **F,** Box plots of cervical tumor mass from mice treated with carboplatin (CP)/paclitaxel (PTX), LPV/r, or LPV/r + carboplatin/paclitaxel, as compared with controls. A significant reduction of tumor mass was evidenced in all treatment groups as compared with controls, as well as in LPV/r versus carboplatin–paclitaxel, and in LPV/r + carboplatin/paclitaxel versus LPV/r or versus carboplatin/paclitaxel-treated mice. Results were analyzed by nonparametric two-tailed, unpaired Mann–Whitney U test ($n = 6$ mice, control; $n = 6$ mice, carboplatin/paclitaxel; $n = 6$ mice, LPV/r; and $n = 5$ mice, LPV/r + carboplatin/paclitaxel).

lesions by an *in situ* gelatin zymography analysis (14). Treatment with IDV/r, SQV/r, or LPV/r significantly reduced MMP activity by 69%, 64%, and 72%, respectively, as compared with control buffer ($P < 0.0001$; **Fig. 4A** and **B**).

Among the various MMPs, MMP-9 plays a prominent role in regulating cervical carcinoma progression and invasion in HPV16/E2 mice, as well as in human cervical carcinoma (15, 17, 25). Therefore, MMP-9 expression was evaluated in mice cervical lesions by real-time RT-PCR analysis. *MMP-9* gene expression was significantly reduced in cervical carcinoma of mice treated with IDV/r, SQV/r, or LPV/r as compared with controls ($P = 0.0003$, $P = 0.002$, and $P = 0.0017$, respectively; **Fig. 4C** and **D**). Results from immunofluorescence analysis performed in LPV/r-treated animals and their controls, indicate that this was associated with a 43% reduction of MMP-9 protein expression ($P < 0.0001$; Supplementary Fig. S2). Thus, treatment with HIV-PIs blocks both MMP-9 expression and activity in HPV16/E2 mice cervical carcinoma lesions.

HIV-PIs restore collagen IV levels in the basement membrane of cervical lesions and of tumor vessels

Because collagen IV is a substrate for MMP-9, cervical lesion sections of mice treated with HIV-PIs or control mice were assessed for collagen IV expression by immunostaining. Cervical carcinoma lesions of control mice were characterized by invading nests of cancer cells without evidence of encirclement by the basement membrane (25, 28) or collagen IV expression (Supplementary Fig. S3). On the contrary, tumors of mice treated with LPV/r (**Fig. 4E**) appeared to be well-encapsulated and expressed significantly higher levels of collagen IV than controls (by 4.9-fold, $P = 0.0051$), without evidence of micro-invasion (28). The same was observed in IDV/r- and SQV/r-treated mice ($P < 0.0001$; Supplementary Fig. S3). In addition, treatment with LPV/r significantly increased the amount of collagen IV by 2.7-fold in the basement membrane of tumor vasculature, as compared with control mice ($P < 0.0001$), therefore, indicating a restoration of the integrity of vascular basement membrane (**Fig. 4F**), one of the determinants of vascular normalization (35). Altogether, these

Published OnlineFirst October 20, 2020; DOI: 10.1158/1535-7163.MCT-20-0055

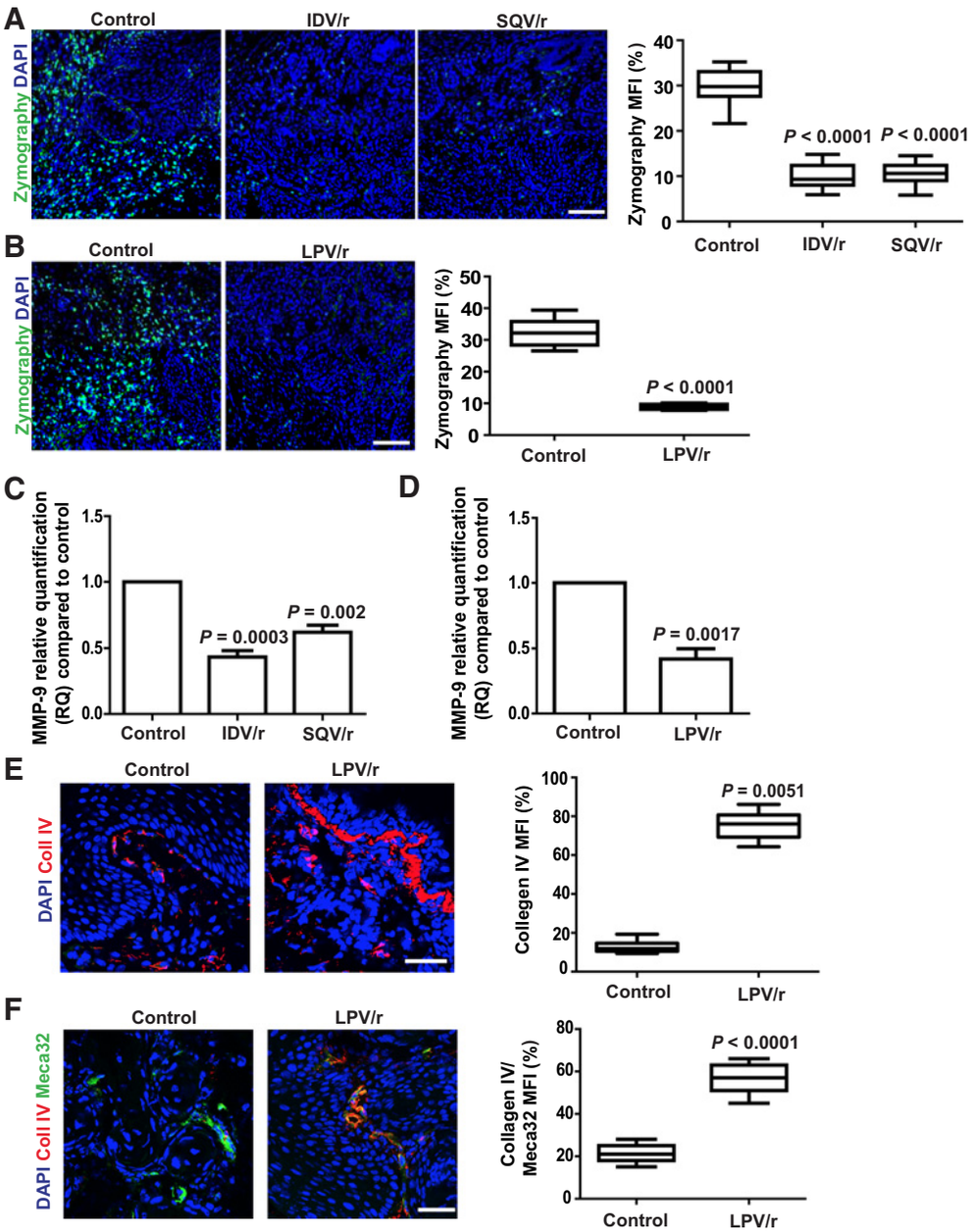

Figure 4.

HIV-PIs inhibit MMP gelatinolytic activity, reduce MMP-9 expression, and restore the basement membrane integrity in HPV16/E2 tumors. **A** and **B,** Confocal images of the *in situ* gelatin zymography (green) of representative cervical sections from mice treated with IDV/r or SQV/r (**A**), LPV/r (**B**), or controls (scale bars, 50 μm). Box plots show the percentage of gelatinolytic area over the total tissue area for IDV/r-, SQV/r-, or LPV/r-treated animals as compared with control mice. Gelatinolytic activity was greatly reduced in all treatment groups as compared with controls, as assessed by the nonparametric two-tailed, unpaired Mann–Whitney U test ($n = 5$ mice/group). **C** and **D,** Real-time RT-PCR quantification of MMP-9 RNA expression in cervical tissues from HPV16/E2 mice. The copy number of MMP-9 RNA molecules from snap-frozen tissue samples of mice treated with IDV/r or SQV/r (**C**), or LPV/r (**D**) was normalized on control. A reduction of *MMP-9* gene expression by 57%, 38%, and 58% was detected in mice treated with IDV/r, SQV/r, or LPV/r, respectively, as compared with control. Results were analyzed by Student *t* test ($n = 3$ mice/group). **E** and **F,** Confocal images of collagen IV expression at the basement membrane of cervical lesions and vessels in representative cervical cross-sections from mice treated with LPV/r or controls. Basement membrane integrity expression was quantified as the percentage of collagen IV–stained area over the total tissue area in the tumor lesions (**E**) or as percentage of colocalization of collagen IV with Meca32 in vessels (**F**). Results were analyzed by nonparametric two-tailed, unpaired Mann–Whitney U test ($n = 3$ mice per group); scale bars, 50 μm.

Published OnlineFirst October 20, 2020; DOI: 10.1158/1535-7163.MCT-20-0055

findings indicate that HIV-PI treatment promotes a reversion of the invasive behavior of cervical carcinoma toward a more benign phenotype.

TIMP-3 expression in HIV-PI–treated HVP16/E2 cervical tumors and in human CIN/cervical carcinoma specimens

The function of MMPs is regulated by the TIMP-1/4 present in most human tissues (38, 39). To further unveil the mechanism for HIV-PI inhibitory effect on MMP activity, *TIMP-1/4* gene expression was evaluated in tumors of treated and control mice by RT-PCR. Treatment with IDV/r, SQV/r, or LPV/r increased TIMP-3 expression by 2.5-, 2.1-, or 2.7-folds, respectively, as compared with control mice ($P = 0.0058$, $P = 0.0036$, $P = 0.0006$, respectively; **Fig. 5A**). Interestingly, this effect occurred in the absence of a significant modulation of the expression of the other TIMPs (Supplementary Fig. S4A–S4C). The effect of HIV-PI treatment on TIMP-3 expression was confirmed at the protein level by immunofluorescence analysis, showing extremely low levels of TIMP-3 protein expression within untreated tumors and a significant increase after IDV/r, SQV/r, and LPV/r treatment ($P < 0.0001$, for all treatment groups; Supplementary Fig. S5A and S5B). We then investigated which components of TME were responsible for the HIV-PI–promoted TIMP-3 expression. By double immunostaining and confocal analysis of LPV/r-treated tumors, we observed a significant increase of TIMP-3 expression in PDGFR-α^+ fibroblasts (**Fig. 5B**), the most abundant cancer-associated fibroblast (CAF) subpopulation present in HPV16/E2 cervical carcinoma (40), and in tumor-associated F4/80$^+$ macrophages (**Fig. 5C**), a tumor-infiltrating immune cell that, by expressing MMP-9, plays a crucial role in HPV16/E2 CIN/cervical carcinoma progression (25), as compared with controls ($P < 0.0001$). Moreover, TIMP-3 expression by Meca32$^+$ vascular cells was significantly higher in LPV/r-treated tumors than in controls (**Fig. 5D**; $P < 0.0001$), suggesting that tumor vessel normalization promoted by HIV-PI treatment was the result of the restoration of the balance between pro- and antiangiogenic molecules.

Because, to be best of our knowledge, there are no reports in the literature about TIMP-3 expression in human CIN/cervical carcinoma lesions, we performed a pilot IHC study to assess TIMP-3 protein levels in human cervical carcinoma specimens as compared with normal cervix and low/high-grade dysplasia, to evaluate the relevance of our experimental findings in human tumors. Remarkably, we observed high levels of TIMP-3 protein expression in normal cervix and a gradual decrease of staining in low- and high-grade dysplastic lesions. Moreover, TIMP-3 was not detectable in cervical carcinoma (**Fig. 5E**). These data are in agreement with our preclinical data showing down modulation of TIMP-3 in mice cervical carcinoma and its overexpression upon LPV/r treatment, and with previous observations indicating increasing MMPs expression/activity both in human lesions and mice during CIN/cervical carcinoma progression (17, 25), further confirming that this model well recapitulates the human disease.

HIV-PI–treated tumors present reduced VEGF/VEGFR complex levels

It has been shown that MMP-9 regulates the angiogenic switch during cancer progression (20) and is able to mobilize VEGF and to increase its association with VEGFR2 in HPV16/E2 mice (25). Moreover, other studies have demonstrated that, independently of its MMP inhibitory activity, TIMP-3 interferes with angiogenesis by directly blocking the binding of VEGF to the VEGFR2 (38). To further investigate the significance of MMP-9 inhibition and TIMP-3 induction by HIV-PIs, HPV16/E2 tumors from treated and control mice were stained with an mAb that specifically recognizes VEGF in complex with VEGFR2 (GVM39) on tumor vasculature (25). Treatment with IDV/r, SQV/r, or LPV/r significantly reduced the levels of the VEGF/VEGFR complex by 82%, 79%, and 85%, respectively, as compared with controls ($P < 0.0001$; **Fig. 6A** and **B**). Taken together, these findings suggest that vessel normalization by HIV-PIs could be due, at least in part, to a blockade of VEGF downstream signaling owing to the inhibition of MMP-9 and upregulation of TIMP-3.

Discussion

Antiretroviral treatment of HIV$^+$ women has reduced the onset and progression of HPV-related uterine cervical lesions, and ultimately the incidence of invasive cervical carcinoma (10, 17). Although part of this effect is conceivably due to the amelioration of the immune response, previous work from us and other groups indicates that HIV-PIs exert direct antitumor and antiangiogenic effects, which are independent of their antiviral activity and may significantly contribute to tumor inhibition and regression (11, 14, 17, 18, 41, 42). This study has examined the effectiveness and the mechanism(s) of action of both first- and second-generation HIV-PIs, including indinavir, saquinavir, and lopinavir, boosted by ritonavir, in a well-established HPV16 E6/E7 transgenic mouse model of spontaneous cervical carcinogenesis (25, 28–30, 43).

Herein, we show that therapeutic doses of HIV-PIs are effective at inhibiting cervical carcinoma progression and tumor-associated angiogenesis, as well as at promoting lesion regression in transgenic mice through several mechanisms that may operate concurrently.

First, HIV-PI treatment was associated with a reduced MMP-9 expression and activity within murine cervical carcinoma. Of note, we have previously demonstrated by genetic knockout or pharmacologic inhibition that MMPs, and in particular MMP-9, play a key role in the development or progression of cervical carcinoma and in the angiogenic switch at the CIN/cervical carcinoma transition (25). In this context, we also showed that HIV-PI concentrations corresponding to the drug peak levels detectable in plasma of treated individuals can efficiently block the growth and invasion of CIN cells through a concomitant reduction of MMP-9 expression and activity by targeting the AKT/Fra-1 signaling pathway (15, 16, 19). This suggests that the inhibition of MMP-9 expression/activity observed upon HIV-PI treatment of HPV16/E2 mice is part of the mechanism by which these drugs impair angiogenesis and tumor progression.

In agreement with the reduced MMP-9 activity promoted by HIV-PIs, we also observed, in treated mice, an increased expression of collagen IV, one of the main ECM substrate of MMP-9, associated with the restoration of ECM at both the epithelial basal layer and endothelial basement membrane. Because loss of collagen IV and membrane integrity are events associated with tumor invasion and metastases (38, 42), these data indicate that HIV-PIs can revert the invasive behavior of cervical lesions of HPV16/E2 mice toward a more benign phenotype.

Noteworthy, a previously unknown effect observed in HIV-PI–treated HPV16/E2 mice was the enhanced expression of the MMP-9 endogenous inhibitor, TIMP-3, concomitantly to the reduction of MMP levels and activity in mice lesion. TIMP-3 behaves as a tumor suppressor and inhibitor of angiogenesis and is downregulated in several tumor types. Interestingly, we also showed here, for the first time, that TIMP-3 is highly expressed in human normal cervix specimens and that its expression is gradually downregulated during CIN/cervical carcinoma progression, indicating that the data obtained in HPV16/E2 mice are relevant for human tumors. It is, therefore, conceivable that the reduced gelatinolytic activity observed in

Published OnlineFirst October 20, 2020; DOI: 10.1158/1535-7163.MCT-20-0055

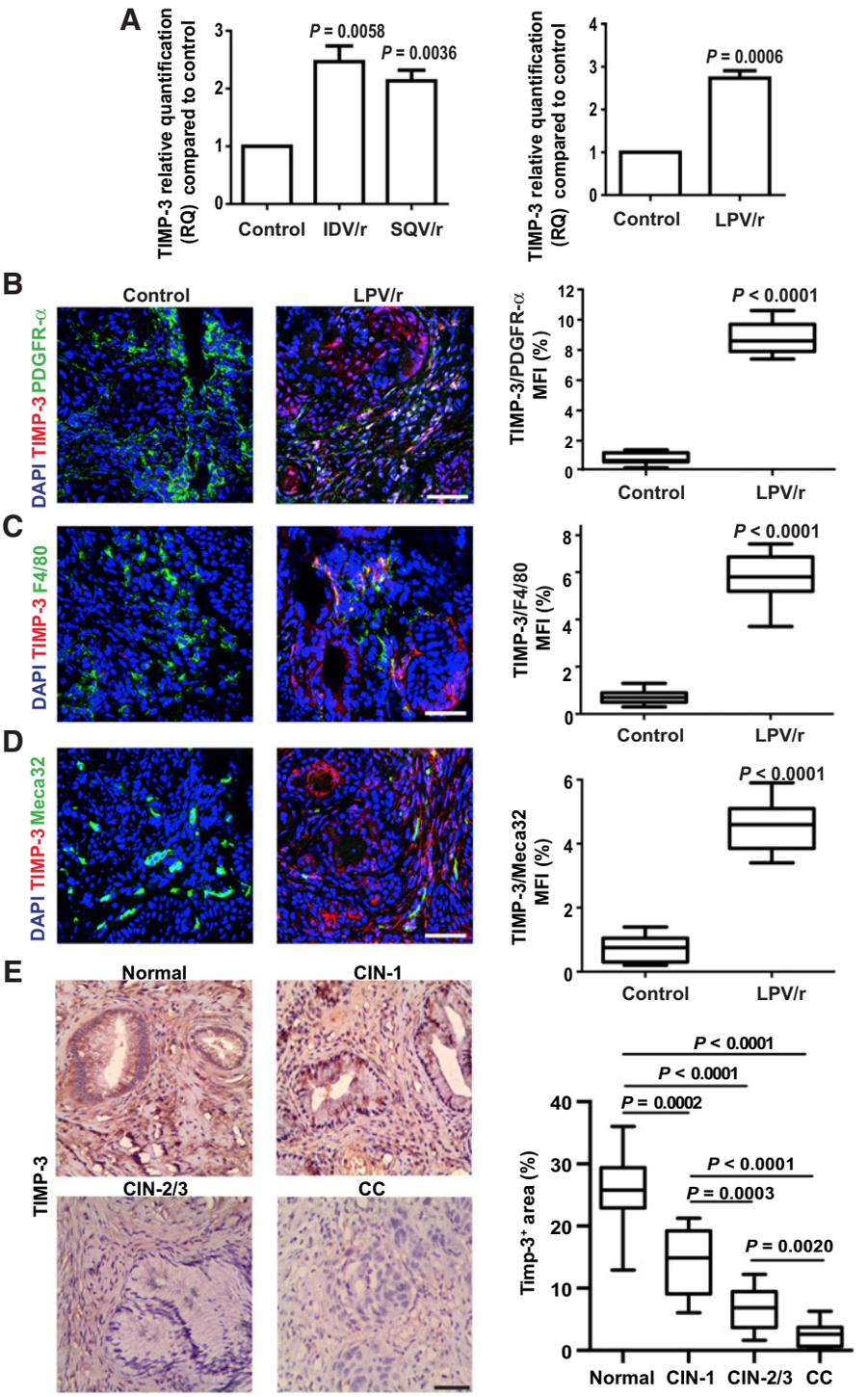

Figure 5.

TIMP-3 expression is increased in tumor cells and TME of HIV-PI–treated tumors and is lost during human CIN/cervical carcinoma (CC) progression. **A,** Real-time RT-PCR quantification of TIMP-3 RNA expression highlights a significant reduction of *TIMP-3* gene expression in cervical tissues from HIV-PI–treated tumors as compared with controls. The copy number of TIMP-3 RNA from snap-frozen tissue samples from mice treated with IDV/r, SQV/r, or LPV/r was normalized on control tumors. Results were analyzed by Student *t* test ($n = 3$ mice/group). Confocal microscopy of TIMP-3 (red channel) and CAFs (PDGFR-α; **B**), macrophages (F4/80; **C**), or vessels (Meca32; green channels; **D**) in representative cervical sections from mice treated LPV/r and control animals (scale bars, 50 μm). Box plots show the percentage of colocalization between TIMP-3 and PDGFR-α or F4/80 or Meca32. TIMP-3 protein expression in fibroblasts, macrophages, and vessels of LPV/r-treaded mice was increased by 10.8-, 7.4-, and 5.7-folds, respectively, as compared with control. Results were analyzed by nonparametric two-tailed, unpaired Mann–Whitney U test ($n = 5$ mice/group). **E,** Immunostaining of TIMP3 protein expression in human cervix specimens. In normal cervix, TIMP-3 presents a diffuse cytoplasmic and nuclear localization within cervical epithelium and cervical stromal cells (fibroblasts and endothelium), which becomes less intense and scattered in CIN-1 lesions. In CIN-2/3 lesions, TIMP-3 only displays a cytoplasmic immunoreactivity in scattered fibroblasts, whereas it is absent in invasive cervical carcinoma. TIMP-3 expression levels are presented as box plots of the percentages of TIMP-3–positive area/field. Results were analyzed by nonparametric two-tailed, unpaired Mann–Whitney U test ($n = 4$ patients/group).

HIV-PI–treated mice may be due, at least in part, to the inhibition of MMP activity by TIMP-3. Of note, a marked reduction of the expression or activity of MMP-inhibiting molecules, including TIMP-1, TIMP-2, and reversion-inducing cysteine-rich protein with Kazal motifs (RECK), was also observed in human invasive/advanced cervical carcinoma, as compared with normal cervical tissue or CIN lesions, in association with increase in MMP-2 and -9 (44).

Consistent with MMP-9 downregulation and TIMP-3 upregulation, HIV-PI–treated mice showed a reduced vessel density associated to a strong decrease of VEGF/VEGFR2 complex in tumors. One explanation of these effects is provided by HIV-PIs' capability of downregulating MMP-9, which may lead to a decreased mobilization of sequestered, ECM-bound VEGF (20, 25), and, at the same time, of upregulating TIMP-3, which is known to block not only the MMP

Published OnlineFirst October 20, 2020; DOI: 10.1158/1535-7163.MCT-20-0055

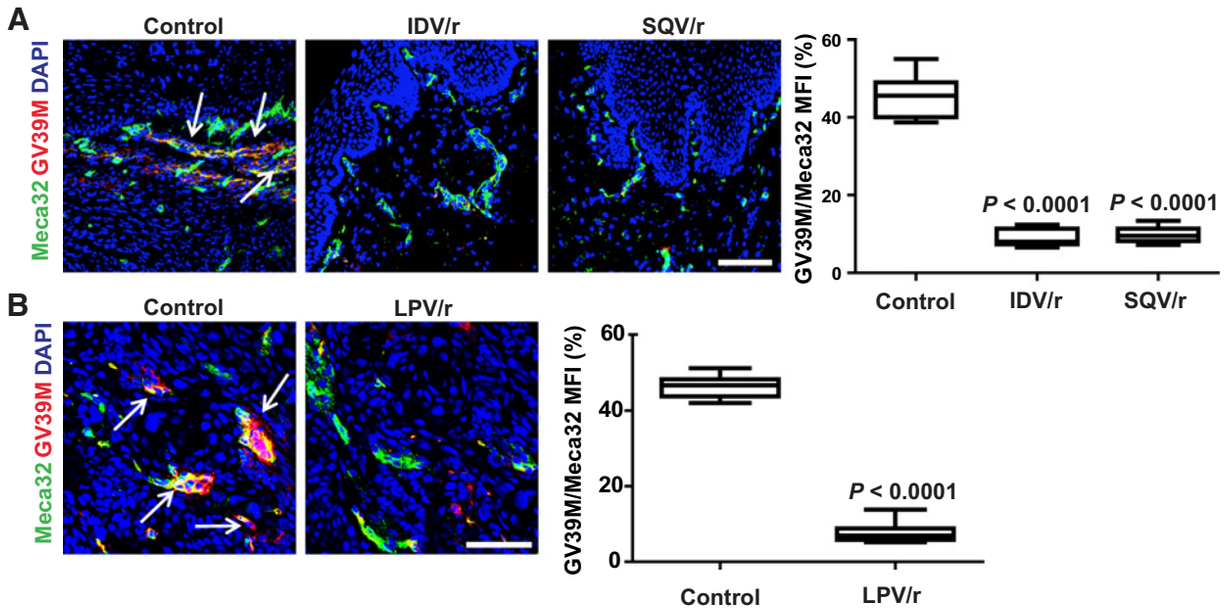

Figure 6.

Tumor vessels of HIV-PI–treated mice present reduced levels of VEGF/VEGFR2 complex. Confocal microscopy of VEGF/VEGFR2 complex assessed by GV39M antibody (red channel) and endothelial cells (EC) visualized with the anti-Meca-32 antibody (green) in representative cervical cross-sections from mice treated with IDV/r or SQV/r (**A**), LPV/r (**B**), or controls (arrows); scale bars, 50 μm. The extent of VEGFR2 occupancy by VEGF in ECs in cervical tissue from mice treated with IDV/r or SQV/r (**A**), or LPV/r (**B**), and control mice are represented as box plots of the percentages of GVM39/Meca32 costaining area over the total tissue area. A significant reduction of the VEGF/VEGFR2 complex was evidenced by nonparametric two-tailed, unpaired Mann–Whitney U test ($n = 5$ mice/group).

catalytic site, but also the VEGF binding to VEGFR2 (38), as observed here.

Although further studies are required to ascertain a causal relationship between HIV-PI antitumor effects and TIMP-3 upregulation in transgenic mice, evidence from the literature indicates that additional mechanisms may also be involved. For instance, the HIV-PIs, nelfinavir and amprenavir, downregulate VEGF expression in tumor cells *in vitro* and *in vivo* by inhibiting the PI3K/Akt pathway (41, 42), which also modulates MMP-9 expression (15, 19). Moreover, HIV-PIs may conceivably interrupt the positive transcriptional feedback loop between VEGF and MMPs (45), which are molecules playing a key role in HPV-promoted cervical tumorigenesis. Indeed, both MMP-9 and VEGF have been shown to be upregulated already in early cervical carcinoma stages of transgenic mice or patients with cervical carcinoma (17, 25) due to the activity of HPV E6 and E7 oncoproteins (46).

Remarkably, our study showed for the first time that HIV-PI antitumor and antiangiogenic effects are associated with the normalization of vessels structure and functionality, as indicated by the increased vessel pericyte coverage and relieve of local tumor hypoxia. In this regard, it is well known that tumor vessels are tortuous, leaky, and poorly covered by pericytes, factors leading not only to tumor hypoxia, which is known to activate several pathways contributing to tumor invasion and metastasis (34, 47–49), but also to low drug penetration into the tumor mass. The factors inducing and sustaining these vessels abnormalities are several, including induction of angiogenic factors (i.e., VEGF) and downregulation of angiogenesis inhibitors, such as TIMPs (35, 37, 43, 44, 50).The impairment of MMP-9 and VEGF availability along with the upregulation of TIMP-3 could represent a mechanism by which HIV-PIs are capable of restoring the balance between pro- and antiangiogenic factors and, consequently, of normalizing the vasculature. However, in addition to this, the endothelial cell–pericyte interaction is known to induce TIMP-3 expression (51), suggesting that the upregulation of TIMP-3 may also be consequent to vessel normalization promoted by HIV-PI treatment. Notably, we observed that in HIV-PI–treated tumors, TIMP-3 expression was increased within different TME cell types playing a key role in CIN/cervical carcinoma progression of HPV16/E2 mice (25, 40). Altogether, these data indicate that the antitumor and antiinvasive effects of HIV-PIs in HPV16/E2 mice may be attributed, at least in part, to their capability of reverting protumoral CAFs, macrophages, and vasculature to a "normalized" phenotype.

These results are of great interest, because it is known that antiangiogenic therapies can result in a worsening of tumor hypoxia, which, in turn, fuels a vicious circle further promoting tumor progression and treatment resistance (34). On the contrary, therapeutic strategies aimed at vessel normalization and at decreasing or preventing tumor hypoxia may overcome the problem of escape resistance to treatment (29, 34, 35, 52). Indeed, the identification of novel targets for tumor vessel normalization is at the forefront of cancer research (30, 34–36, 53). In this context, the anti-VEGF mAb, bevacizumab, has demonstrated clinical efficacy in recurrent and metastatic cervical carcinoma when combined with conventional chemotherapy, and is now the first biologic drug approved for use in late-stage cervical carcinoma (54), indicating that treatments aimed at targeting tumor vasculature could represent a novel and alternative therapeutic strategy in cervical carcinoma. Remarkably, in our study, HIV-PIs used as single agent not only impaired invasive cervical carcinoma, but normalized tumor vasculature and significantly reduced tumor hypoxia, suggesting that these drugs, by acting on TME, could prevent or overcome tumor cell resistance to treatments. In agreement with this hypothesis, we showed here that HIV-PIs not only have more potent antitumor effects in HPV16/E2 mice as compared with the standard-

Published OnlineFirst October 20, 2020; DOI: 10.1158/1535-7163.MCT-20-0055

of-care regimen for cervical carcinoma, but also enhanced chemotherapy antitumor activity, without additional toxicity.

Finally, in this study, we also observed a reduction of Ki67 expression in HIV-PI–treated mice, which is a marker of poor prognosis for women with cervical carcinoma (32), and they increased apoptosis within the tumor mass and tumor vessels. Previous studies indicated that the induction of apoptosis in endothelial or cancer cells, including cervical carcinoma cells and HPV16-immortalized and -transformed cells, occurred only at molar concentrations of HIV-PIs, which are much higher than those used here and measured in plasma of HIV^+-treated patients, likely through a proteasome-mediated mechanism(s) involving p53 stabilization and upregulation of the antiviral protein ribonuclease L, and with different potency by the different HIV-PIs (11, 13–15, 17, 21). This suggests that the enhanced apoptosis observed in HIV-PI–treated transgenic mice may be due to other mechanisms, such as TIMP-3 induction (55, 56) and/or inhibition of VEGF signaling (33).

Despite worldwide campaigns for screening programs for the detection and surveillance of CIN lesions and for a global coverage against HPV by preventative vaccination, the burden of HPV^+ women at risk of CIN/cervical carcinoma development currently remains very high, particularly in low-resource settings. Furthermore, no therapies are available to eradicate or block persistent HR-HPV infection, the cause of nearly 100% of all cervical carcinomas. There is, therefore, a strong need for new approaches against HR-HPV and cervical carcinoma capable of preventing CIN progression, and to develop effective and tolerable second-line therapies in advanced cervical carcinoma. In this context, HIV-PIs may represent a new alternative intervention to current invasive treatments for CIN, including surgical interventions, which are often accompanied by short-term (local hemorrhage, infections, and lesion of proximal organs) or long-term (cervical stenosis, infertility, and preterm births) side effects or lesion persistence/recurrence (57, 58).

Several trials conducted with HIV-PIs in patients with cancer, including HIV-negative Kaposi sarcoma or CIN (23, 24), indicated that HIV-PIs have good tolerability and promising antitumor activity. Our results may also open perspectives for new dosing and delivery systems, including drug formulations for topical therapy to locally achieve persistently high drug concentrations promoting proteasome-mediated HIV-PI effects (13, 17), leading to simplified treatments that may benefit HIV^+ or seronegative men and women at risk of HPV-associated cancers. In addition, based on their capability of normalizing tumor vessel, these drugs could be combined with conventional cytotoxic antitumor drugs or other targeted immunotherapy thus, addressing the unmet clinical need for effective and tolerable second-line therapies in advanced cervical carcinoma (54). Most HIV-PIs are already available as generic drugs thus, HIV-PI drug repositioning for cervical carcinoma therapy may strongly impact the costs for national health systems, particularly in developing countries. Because HIV-PIs are already in clinical use, and have a well-known toxicological and pharmacologic profile, these results may rapidly provide strong indications for their use in women with CIN/cervical carcinoma infected or noninfected by HIV.

Disclosure of Potential Conflicts of Interest

G. Barillari reports grants from Italian Ministry of Health (a research grant which financed laboratory reagents, and was provided by the Italian government) during the conduct of the study. No potential conflicts of interest were disclosed by the other authors.

Authors' Contributions

Y. Qiu: Data curation, formal analysis, validation, investigation, methodology, writing-original draft, writing-review and editing. **F. Maione:** Data curation, formal analysis, validation, investigation, methodology, writing-original draft, writing-review and editing. **S. Capano:** Data curation, formal analysis, investigation. **C. Meda:** Data curation, formal analysis, investigation. **O. Picconi:** Data curation, formal analysis, validation, writing-original draft. **S. Brundu:** Data curation, formal analysis, validation, investigation, methodology, writing-review and editing. **A. Pisacane:** Resources, validation, interpretation of histopathologic studies. **A. Sapino:** Resources, validation, interpretation of histopathologic studies. **C. Palladino:** Data curation, formal analysis. **G. Barillari:** Conceptualization, writing-original draft, writing-review and editing. **P. Monini:** Conceptualization, supervision, methodology, writing-original draft, writing-review and editing. **F. Bussolino:** Funding acquisition, writing-original draft, writing-review and editing. **B. Ensoli:** Conceptualization, supervision, funding acquisition, writing-review and editing. **C. Sgadari:** Conceptualization, resources, data curation, supervision, funding acquisition, validation, visualization, methodology, writing-original draft, writing-review and editing. **E. Giraudo:** Conceptualization, resources, formal analysis, supervision, funding acquisition, validation, visualization, methodology, writing-original draft, project administration, writing-review and editing.

Acknowledgments

This work was supported by the Italian Ministry of Health, Programma Straordinario di Ricerca Oncologica (to B. Ensoli, G. Barillari, and E. Giraudo) and Programma Nazionale AIDS (to B. Ensoli and C. Sgadari); Associazione Italiana per la Ricerca sul Cancro (AIRC, to B. Ensoli); Merck Italia Inc. (to B. Ensoli); Agenzia Italiana del Farmaco (AIFA, to B. Ensoli); Associazione Italiana per la Ricerca sul Cancro (AIRC), IG-15645 and IG-19957 (to E. Giraudo); Fondazione Piemontese per la Ricerca sul Cancro (FPRC), FPRC-5 per Mille 2014 Ministero Salute (to E. Giraudo); AIRC 5 per Mille, Special Program on Metastatic Disease (#21052, to E. Giraudo); ERA-Net Transcan-2-JTC 2017 (TOPMESO, to F. Bussolino); AIRC (IG-18652 and IG-12182, to F. Bussolino); Ministry of University and Research (grant 2017237P5X to F. Bussolino); and Swiss National Science Foundation, Sinergia grant no. CRSII3 160742/1 (to E. Giraudo). We wish to thank M. Falchi and S. Moretti for helpful discussion, and F. Cammisa for editorial assistance.

The costs of publication of this article were defrayed in part by the payment of page charges. This article must therefore be hereby marked *advertisement* in accordance with 18 U.S.C. Section 1734 solely to indicate this fact.

Received January 22, 2020; revised July 9, 2020; accepted October 1, 2020; published first October 20, 2020.

References

1. Bodily J, Laimins LA. Persistence of human papillomavirus infection: keys to malignant progression. Trends Microbiol 2011;19:33–9.
2. Rositch AF, Koshiol J, Hudgens MG, Razzaghi H, Backes DM, Pimenta JM, et al. Patterns of persistent genital human papillomavirus infection among women worldwide: a literature review and meta-analysis. Int J Cancer 2013;133:1271–85.
3. Dall KL, Scarpini CG, Roberts I, Winder DM, Stanley MA, Muralidhar B, et al. Characterization of naturally occurring HPV16 integration sites isolated from cervical keratinocytes under noncompetitive conditions. Cancer Res 2008;68:8249–59.
4. Kreimer AR, Schiffman M, Herrero R, Hildesheim A, González P, Burk RD, et al. Long-term risk of recurrent cervical human papillomavirus infection and precancer and cancer following excisional treatment. Int J Cancer 2012;131:211–8.
5. Arbyn M, Redman CWE, Verdoodt F, Kyrgiou M, Tzafetas M, Ghaem-Maghami S, et al. Incomplete excision of cervical precancer as a predictor of treatment failure: a systematic review and meta-analysis. Lancet Oncol 2017;18:1665–79.
6. Forman D, de Martel C, Lacey CJ, Soerjomataram I, Lortet-Tieulent J, Bruni L, et al. Global burden of human papillomavirus and related diseases. Vaccine 2012;30:F12–23.

7. Bruni L, Diaz M, Castellsagué X, Ferrer E, Bosch FX, de Sanjosé S. Cervical human papillomavirus prevalence in 5 continents: meta-analysis of 1 million women with normal cytological findings. J Infect Dis 2010;202:1789–99.
8. Ferlay J, Soerjomataram I, Dikshit R, Eser S, Mathers C, Rebelo M, et al. Cancer incidence and mortality worldwide: sources, methods and major patterns in GLOBOCAN 2012. Int J Cancer 2015;136:E359–86.
9. Blitz S, Baxter J, Raboud J, Walmsley S, Rachlis A, Smaill F, et al. Evaluation of HIV and highly active antiretroviral therapy on the natural history of human papillomavirus infection and cervical cytopathologic findings in HIV-positive and high-risk HIV-negative women. J Infect Dis 2013;208:454–62.
10. Kelly H, Weiss HA, Benavente Y, de Sanjose S, Mayaud P, Group ART, et al. Association of antiretroviral therapy with high-risk human papillomavirus, cervical intraepithelial neoplasia, and invasive cervical cancer in women living with HIV: a systematic review and meta-analysis. Lancet HIV 2018;5:e45–58.
11. Sgadari C, Barillari G, Toschi E, Carlei D, Bacigalupo I, Baccarini S, et al. HIV protease inhibitors are potent anti-angiogenic molecules and promote regression of Kaposi sarcoma. Nat Med 2002;8:225–32.
12. Sgadari C, Monini P, Barillari G, Ensoli B. Use of HIV protease inhibitors to block Kaposi's sarcoma and tumour growth. Lancet Oncol 2003;4:537–47.
13. Monini P, Sgadari C, Toschi E, Barillari G, Ensoli B. Antitumour effects of antiretroviral therapy. Nat Rev Cancer 2004;4:861–75.
14. Toschi E, Sgadari C, Malavasi L, Bacigalupo I, Chiozzini C, Carlei D, et al. Human immunodeficiency virus protease inhibitors reduce the growth of human tumors via a proteasome-independent block of angiogenesis and matrix metalloproteinases. Int J Cancer 2011;128:82–93.
15. Barillari G, Iovane A, Bacigalupo I, Palladino C, Bellino S, Leone P, et al. Ritonavir or saquinavir impairs the invasion of cervical intraepithelial neoplasia cells via a reduction of MMP expression and activity. AIDS 2012;26:909–19.
16. Barillari G, Iovane A, Bacigalupo I, Labbaye C, Chiozzini C, Sernicola L, et al. The HIV protease inhibitor indinavir down-regulates the expression of the pro-angiogenic MT1-MMP by human endothelial cells. Angiogenesis 2014;17:831–8.
17. Barillari G, Monini P, Sgadari C, Ensoli B. The impact of human papilloma viruses, matrix metallo-proteinases and HIV protease inhibitors on the onset and progression of uterine cervix epithelial tumors: a review of preclinical and clinical studies. Int J Mol Sci 2018;19:1418.
18. Esposito V, Palescandolo E, Spugnini EP, Montesarchio V, De Luca A, Cardillo I, et al. Evaluation of antitumoral properties of the protease inhibitor indinavir in a murine model of hepatocarcinoma. Clin Cancer Res 2006;12:2634–9.
19. Bacigalupo I, Palladino C, Leone P, Toschi E, Sgadari C, Ensoli B, et al. Inhibition of MMP-9 expression by ritonavir or saquinavir is associated with inactivation of the AKT/Fra-1 pathway in cervical intraepithelial neoplasia cells. Oncol Lett 2017;13:2903–8.
20. Bergers G, Brekken R, McMahon G, Vu TH, Itoh T, Tamaki K, et al. Matrix metalloproteinase-9 triggers the angiogenic switch during carcinogenesis. Nat Cell Biol 2000;2:737–44.
21. Hampson L, Kitchener HC, Hampson IN. Specific HIV protease inhibitors inhibit the ability of HPV16 E6 to degrade p53 and selectively kill E6-dependent cervical carcinoma cells in vitro. Antivir Ther 2006;11:813–25.
22. Batman G, Oliver AW, Zehbe I, Richard C, Hampson L, Hampson IN. Lopinavir up-regulates expression of the antiviral protein ribonuclease L in human papillomavirus-positive cervical carcinoma cells. Antivir Ther 2011;16:515–25.
23. Monini P, Sgadari C, Grosso MG, Bellino S, Di Biagio A, Toschi E, et al. Clinical course of classic Kaposi's sarcoma in HIV-negative patients treated with the HIV protease inhibitor indinavir. AIDS 2009;23:534–8.
24. Hampson L, Maranga IO, Masinde MS, Oliver AW, Batman G, He X, et al. A single-arm, proof-of-concept trial of lopimune (lopinavir/ritonavir) as a treatment for HPV-related pre-invasive cervical disease. PLoS One 2016;11: e0147917.
25. Giraudo E, Inoue M, Hanahan D. An amino-bisphosphonate targets MMP-9-expressing macrophages and angiogenesis to impair cervical carcinogenesis. J Clin Invest 2004;114:623–33.
26. Dobbs SP, Hewett PW, Johnson IR, Carmichael J, Murray JC. Angiogenesis is associated with vascular endothelial growth factor expression in cervical intraepithelial neoplasia. Br J Cancer 1997;76:1410–5.
27. Arbeit JM, Howley PM, Hanahan D. Chronic estrogen-induced cervical and vaginal squamous carcinogenesis in human papillomavirus type 16 transgenic mice. Proc Natl Acad Sci U S A 1996;93:2930–5.
28. Riley RR, Duensing S, Brake T, Münger K, Lambert PF, Arbeit JM. Dissection of human papillomavirus E6 and E7 function in transgenic mouse models of cervical carcinogenesis. Cancer Res 2003;63:4862–71.
29. Maione F, Capano S, Regano D, Zentilin L, Giacca M, Casanovas O, et al. Semaphorin 3A overcomes cancer hypoxia and metastatic dissemination induced by antiangiogenic treatment in mice. J Clin Invest 2012;122: 1832–48.
30. Maione F, Molla F, Meda C, Latini R, Zentilin L, Giacca M, et al. Semaphorin 3A is an endogenous angiogenesis inhibitor that blocks tumor growth and normalizes tumor vasculature in transgenic mouse models. J Clin Invest 2009;119: 3356–72.
31. Ragnum HB, Vlatkovic L, Lie AK, Axcrona K, Julin CH, Frikstad KM, et al. The tumour hypoxia marker pimonidazole reflects a transcriptional programme associated with aggressive prostate cancer. Br J Cancer 2015;112:382–90.
32. Pan D, Wei K, Ling Y, Su S, Zhu M, Chen G. The prognostic role of Ki-67/MIB-1 in cervical cancer: a systematic review with meta-analysis. Med Sci Monit 2015; 21:882–9.
33. Epstein RJ. VEGF signaling inhibitors: more pro-apoptotic than anti-angiogenic. Cancer Metastasis Rev 2007;26:443–52.
34. Jain RK. Antiangiogenesis strategies revisited: from starving tumors to alleviating hypoxia. Cancer Cell 2014;26:605–22.
35. Martin JD, Seano G, Jain RK. Normalizing function of tumor vessels: progress, opportunities, and challenges. Annu Rev Physiol 2019;81:505–34.
36. De Bock K, Cauwenberghs S, Carmeliet P. Vessel abnormalization: another hallmark of cancer? Molecular mechanisms and therapeutic implications. Curr Opin Genet Dev 2011;21:73–9.
37. Carmeliet P, Jain RK. Molecular mechanisms and clinical applications of angiogenesis. Nature 2011;473:298–307.
38. Bourboulia D, Stetler-Stevenson WG. Matrix metalloproteinases (MMPs) and tissue inhibitors of metalloproteinases (TIMPs): positive and negative regulators in tumor cell adhesion. Semin Cancer Biol 2010;20:161–8.
39. Jackson HW, Defamie V, Waterhouse P, Khokha R. TIMPs: versatile extracellular regulators in cancer. Nat Rev Cancer 2017;17:38–53.
40. Pietras K, Pahler J, Bergers G, Hanahan D. Functions of paracrine PDGF signaling in the proangiogenic tumor stroma revealed by pharmacological targeting. PLoS Med 2008;5:e19.
41. Pore N, Gupta AK, Cerniglia GJ, Jiang Z, Bernhard EJ, Evans SM, et al. Nelfinavir down-regulates hypoxia-inducible factor 1alpha and VEGF expression and increases tumor oxygenation: implications for radiotherapy. Cancer Res 2006; 66:9252–9.
42. Pore N, Gupta AK, Cerniglia GJ, Maity A. HIV protease inhibitors decrease VEGF/HIF-1alpha expression and angiogenesis in glioblastoma cells. Neoplasia 2006;8:889–95.
43. Smith-McCune K, Zhu YH, Hanahan D, Arbeit J. Cross-species comparison of angiogenesis during the premalignant stages of squamous carcinogenesis in the human cervix and K14-HPV16 transgenic mice. Cancer Res 1997;57:1294–300.
44. Cardeal LB, Boccardo E, Termini L, Rabachini T, Andreoli MA, di Loreto C, et al. HPV16 oncoproteins induce MMPs/RECK-TIMP-2 imbalance in primary keratinocytes: possible implications in cervical carcinogenesis. PLoS One 2012;7:e33585.
45. Hollborn M, Stathopoulos C, Steffen A, Wiedemann P, Kohen L, Bringmann A. Positive feedback regulation between MMP-9 and VEGF in human RPE cells. Invest Ophthalmol Vis Sci 2007;48:4360–7.
46. Toussaint-Smith E, Donner DB, Roman A. Expression of human papillomavirus type 16 E6 and E7 oncoproteins in primary foreskin keratinocytes is sufficient to alter the expression of angiogenic factors. Oncogene 2004;23:2988–95.
47. Pàez-Ribes M, Allen E, Hudock J, Takeda T, Okuyama H, Viñals F, et al. Antiangiogenic therapy elicits malignant progression of tumors to increased local invasion and distant metastasis. Cancer Cell 2009;15:220–31.
48. Sennino B, McDonald DM. Controlling escape from angiogenesis inhibitors. Nat Rev Cancer 2012;12:699–709.
49. Ebos JM, Lee CR, Kerbel RS. Tumor and host-mediated pathways of resistance and disease progression in response to antiangiogenic therapy. Clin Cancer Res 2009;15:5020–5.
50. Hanahan D, Folkman J. Patterns and emerging mechanisms of the angiogenic switch during tumorigenesis. Cell 1996;86:353–64.
51. Saunders WB, Bohnsack BL, Faske JB, Anthis NJ, Bayless KJ, Hirschi KK, et al. Coregulation of vascular tube stabilization by endothelial cell TIMP-2 and pericyte TIMP-3. J Cell Biol 2006;175:179–91.
52. Sennino B, Ishiguro-Oonuma T, Wei Y, Naylor RM, Williamson CW, Bhagwandin V, et al. Suppression of tumor invasion and metastasis by concurrent inhibition of c-Met and VEGF signaling in pancreatic neuroendocrine tumors. Cancer Discov 2012;2:270–87.

Published OnlineFirst October 20, 2020; DOI: 10.1158/1535-7163.MCT-20-0055

53. Serini G, Bussolino F, Maione F, Giraudo E. Class 3 semaphorins: physiological vascular normalizing agents for anti-cancer therapy. J Intern Med 2013;273:138–55.
54. Krill LS, Tewari KS. Exploring the therapeutic rationale for angiogenesis blockade in cervical cancer. Clin Ther 2015;37:9–19.
55. Baker AH, George SJ, Zaltsman AB, Murphy G, Newby AC. Inhibition of invasion and induction of apoptotic cell death of cancer cell lines by overexpression of TIMP-3. Br J Cancer 1999;79:1347–55.
56. Qi JH, Anand-Apte B. Tissue inhibitor of metalloproteinase-3 (TIMP3) promotes endothelial apoptosis via a caspase-independent mechanism. Apoptosis 2015;20:523–34.
57. Prendiville W. The treatment of CIN: what are the risks? Cytopathology 2009;20:145–53.
58. Sadler L, Saftlas A. Cervical surgery and preterm birth. J Perinat Med 2007;35:5–9.

Published OnlineFirst October 20, 2020; DOI: 10.1158/1535-7163.MCT-20-0055

Molecular Cancer Therapeutics

HIV Protease Inhibitors Block HPV16-Induced Murine Cervical Carcinoma and Promote Vessel Normalization in Association with MMP-9 Inhibition and TIMP-3 Induction

Yaqi Qiu, Federica Maione, Stefania Capano, et al.

Mol Cancer Ther 2020;19:2476-2489. Published OnlineFirst October 20, 2020.